BIMANES
VIII: PHOTOPHYSICAL PROPERTIES OF *syn*- AND *anti*-1,5-
DIAZABICYCLO[3.3.0]OCTADIENEDIONES (9,10-DIOXABIMANES)

EDWARD M. KOSOWER[†], HANNAH KANETY and HANNA DODIUK

Department of Chemistry, Tel Aviv University, Ramat Aviv, Tel Aviv 69978 (Israel)

(Received January 30, 1982; in revised form July 2, 1982)

Summary

Photophysical data for *syn*- and *anti*-1,5-diazabicyclo[3.3.0]octadiene-diones (9,10-dioxabimanes ((R_2,R_1)B)), a new class of small heterocyclic molecules, are reported. The *syn* and *anti* isomers differ greatly in the positions of the absorption maxima ($\lambda_{max}(syn) > \lambda_{max}(anti)$), the solvent sensitivities of the absorption maxima (that of the *syn* isomer is greater than that of the *anti* isomer), the fluorescence quantum yields ($\phi_F(syn) \gg \phi_F(anti)$), the phosphorescence quantum yields ($\phi_P(syn) \ll \phi_P(anti)$), but they exhibit similar changes in some of these properties with respect to changes in substitution. The 4,6-bridged *syn*-bimanes absorb at shorter wavelengths than unbridged compounds do, but they fluoresce at similar wavelengths. The phosphorescence of the *anti*-(R_2,R_1)B appears at shorter wavelengths and has a somewhat shorter lifetime than that of the corresponding *syn*-(R_2,R_1)B.

1. Introduction

The 1,5-diazabicyclo[3.3.0]octadienediones (9,10-dioxabimanes) ((R_2,R_1)B) first attracted our attention through the strikingly beautiful fluoresence of the *syn* isomers. This aesthetically pleasing physical phenomenon, together with its contrast to the weak fluorescence and strong phosphorescence of the isomeric 9,10-dioxa-*anti*-bimanes [1], was a natural stimulus for a careful study of the photophysical properties of these molecules. Effective syntheses and transformations made many interesting variations on the molecular structures possible [1 - 4]. 9,10-dioxa-*syn*-bimane derivatives are extremely useful fluorescent labeling agents for cells and proteins [5 - 8], emphasizing the need for detailed photophysical analysis. In addition, the bimanes represent novel and unusually small doubly conjugated systems which have proved to be extremely rewarding in the investi-

---

[†]Also at Department of Chemistry, State University of New York, Stony Brook, NY 11794, U.S.A.

gation of a variety of photochemical and photophysical phenomena [9 - 16]. We now report additional absorption and emission data on the *syn*- and *anti*-9,10-dioxabimanes (*cf.* refs. 2 and 4 for previous studies). Syntheses of several new bimanes are also reported.

syn − (R₂,Rᵢ)B   anti − (R₂,Rᵢ)B

1   2

2. Experimental details

2.1. Materials

Most of the compounds for which photophysical data are reported have been described previously [2]. The syntheses and properties of a number of new compounds are given below.

2.1.1. 9,10-dioxa-syn-(methyl,tert-butyl)bimane (3,7-di-tert-butyl-4,6-dimethyl-1,5-diazabicyclo[3.3.0]octa-3,6-diene-2,8-dione)

Ethyl α-*tert*-butylacetoacetate [17] (6.0 g, 32 mmol) was refluxed with hydrazine hydrate (1.62 g, 33 mmol) in ethanol (50 ml) for 16 h, and the solvent was removed; the residue was heated at 70 °C for 3 h at 0.1 Torr and then crystallized from ethanol:ether (2:1) to yield 3-methyl-4-*tert*-butyl-2-pyrazolin-5-one (4.4 g (89%); melting point, 190 °C). The IR spectrum (KBr) is as follows: 3370, 3000 - 2500 (very broad), 1590, 1500, 1450, 1340, 1240 and 1110 cm⁻¹. The ¹H nuclear magnetic resonance (NMR) spectrum (solvent, CDCl₃) shows the following bands in parts per million: 1.30, singlet (9 H); 2.22, singlet (3 H); 6.9, broad singlet (1 H). The pyrazolinone (1.5 g, 10 mmol) was treated in 1,2-dichloroethane (10 ml) with a slow stream of chlorine until the material had dissolved to give a greenish yellow solution. The chlorine was removed with a stream of air, the solvent was evaporated and the residue was crystallized from toluene−petroleum ether (boiling point range, 40 - 60 °C) to yield white crystals of 3-methyl-4-*tert*-butyl-4-chloro-2-pyrazolin-5-one (1.45 g (74%); melting point, 166 °C). The IR spectrum (KBr) is as follows: 3210, 2970, 1710, 1605, 1425, 1370, 1280 and 1230 cm⁻¹. The ¹H NMR spectrum (solvent, CDCl₃) shows the following bands in parts per million: 1.15, singlet (9 H); 2.21, singlet (3 H); 9.55, broad singlet (1 H). The chloropyrazolinone (0.7 g, 3.7 mmol) and K₂CO₃·$\frac{3}{2}$H₂O (1.5 g, 9.1 mmol) were stirred together in CH₂Cl₂ (30 ml) for 72 h, the suspension was filtered through Celite, the solvent was evaporated and

the residue was crystallized from toluene–petroleum ether (boiling point range, 60 - 80 °C) to yield a yellow solid, syn-(CH$_3$,(CH$_3$)$_3$C)B (70 mg (12%); melting point, 218 °C). The IR spectrum (KBr) is as follows: 2960, 1740, 1670, 1590, 1410, 1255 and 1140 cm^{-1}. The ^{1}H NMR spectrum (solvent, CDCl$_3$) shows the following bands in parts per million: 1.30, singlet (9 H); 2.40, singlet (3 H). The UV spectrum (solvent, dioxane) (λ_{max}) is as follows: 370 nm (ϵ = 8000); 255 nm (ϵ = 4800) (shoulder); 232 nm (ϵ = 13 000). The fluorescence spectrum (solvent, dioxane) (λ_{max}) consists of bands at 426 and 450 nm (shoulder) (ϕ_F = 0.80). The peak in the mass spectrum (M^+) is at 276.

2.1.2. 9,10-dioxa-syn-(4-chlorophenyl,methyl)bimane

Ethyl α-methyl-4-chlorobenzoyl acetate (obtained from ethyl hydrogen methyl malonate and 4-chlorobenzoyl chloride (yield, 42%) according to a procedure for 4-nitrobenzoyl chloride [18]) (boiling point at 0.1 Torr, 106 - 108 °C) was converted (yield, 66%) to the pyrazolinone (melting point, 222 °C). The ^{1}H NMR spectrum (solvent, dimethylsulfoxide-d_6) shows the following bands in parts per million: 2.00, singlet (3 H); 7.65, broad singlet (4 H). Chlorination was effected (yield, 54%) in the same way as described for the tert-butyl derivative (above), the product (melting point, 128 - 129 °C) being recrystallized from benzene. The ^{1}H NMR spectrum (solvent, CDCl$_3$) shows the following bands in parts per million: 1.96, singlet (3 H); 7.45, singlet (2 H); 7.95, singlet (2 H); 8.08, singlet (2 H); 9.30, broad singlet (1 H). Conversion to the syn-bimane, syn-(4-ClC$_6$H$_4$,CH$_3$)B (yellow solid; melting point, 310 °C; crystallized from CH$_3$CN), was effected (yield, 28%) with K$_2$CO$_3$·$\frac{3}{2}$H$_2$O. The IR spectrum (KBr) is as follows: 2920, 1780, 1750, 1660, 1630, 1590, 1490, 1415 and 1230 cm^{-1}. The ^{1}H NMR spectrum (solvent, CDCl$_3$) shows the following bands in parts per million: 1.79, singlet (3 H); 6.92, singlet; 7.04, singlet; 7.13, singlet; 7.25, singlet (4 H). The UV spectrum (solvent, dioxane) (λ_{max}) is as follows: 358 nm (ϵ = 5500); 269 nm (ϵ = 17 800); 220 nm (ϵ = 19 800). The fluorescence spectrum (solvent, dioxane) (λ_{max}) consists of bands at 446 and 470 nm (shoulder) (ϕ_F = 0.87). Analyses for C$_{20}$H$_{14}$Cl$_2$N$_2$O$_2$ gave the following results: calculated, 62.24 C, 3.85 H and 7.22 N; found, 62.02 C, 4.13 H and 7.24 N.

2.1.3. 9,10-dioxa-syn-(4-methoxyphenyl,methyl)bimane

This compound was prepared by the K$_2$CO$_3$·$\frac{3}{2}$H$_2$O–CH$_2$Cl$_2$ procedure (yield, 36%) from 3-(4-methoxyphenyl)-4-bromo-4-methyl-2-pyrazolin-5-one [19] to give syn-(4-CH$_3$OC$_6$H$_4$,CH$_3$)B (deep yellow crystals; melting point, 239 °C; crystallized from CH$_3$CN). The IR spectrum (KBr) is as follows: 3060, 2930, 1780 (shoulder), 1745, 1660, 1515, 1415 and 1185 cm^{-1}. The ^{1}H NMR spectrum (solvent, CDCl$_3$) shows the following bands in parts per million: 1.80, singlet (3 H); 3.72, singlet (3 H); 6.52 - 7.00, multiplet (4 H). The UV spectrum (solvent, dioxane) (λ_{max}) is as follows: 358 nm (ϵ = 5400); 280 nm (ϵ = 15 700); 220 nm (ϵ = 18 000). The fluorescence spectrum

(solvent, dioxane) (λ_{max}) consists of bands at 446 and 475 nm (shoulder) ($\phi_F = 0.58$). The peak in the mass spectrum (chemical ionization) (($M + 1)^+$) is at 377. Analyses for $C_{22}H_{24}N_2O_4$ gave the following results: calculated, 70.20 C, 5.36 H and 7.44 N; found, 69.70 C, 5.26 H and 7.04 N.

2.1.4. 9,10-dioxa-syn-(4-nitrophenyl,phenyl)bimane

Methyl *trans*-α-phenyl-4-nitrocinnamate [20] was converted to the pyrazolidinone by refluxing with excess hydrazine hydrate in ethanol for 20 h (yield, 70%; melting point, 112 °C; crystallized from 2-propanol). The ^{1}H NMR spectrum shows the following bands in parts per million: 3.95, doublet (1 H); 4.92, doublet (1 H); 7.49, broad singlet (7 H); 7.72, singlet (7 H); 8.30, singlet (2 H); 8.45, singlet (2 H). The chloro derivative was produced by chlorination in CH_2Cl_2 (yield, 91%; melting point, 165 - 167 °C; crystallized from benzene–petroleum ether (boiling point range, 40 - 60 °C)). Treatment of the chloro derivative with $K_2CO_3 \cdot \frac{3}{2}H_2O$ in CH_2Cl_2 gave the dioxabimane *syn*-(4-$NO_2C_6H_4$,C_6H_5)B (yellow solid; yield, 2.3%; melting point, 312 °C; crystallized from CH_3CN). The IR spectrum (KBr) is as follows: 1745, 1675, 1605, 1525, 1400, 1355, 1240 and 1060 cm^{-1}. The UV spectrum (solvent, dioxane) (λ_{max}) is as follows: 415 nm ($\epsilon = 10\,900$); 297 nm ($\epsilon = 13\,700$); 255 nm ($\epsilon = 29\,600$). The fluorescence spectrum (dioxane) (λ_{max}) consists of bands at 520 and 550 nm (shoulder) ($\phi_F = 0.28$). The peak in the mass spectrum (M^+) is at 530.

2.2. Solvents

Dioxane, isopentane, benzene, acetonitrile, methanol, diethyl ether and tetrachloromethane were spectroscopic grade solvents, obtained from E. Merck, Darmstadt. The ethanol was AnalaR grade (obtained from E. Merck, Darmstadt). The water was triply distilled.

2.3. Solvent polarity parameters

The $E_T(30)$ value was measured, if necessary [21 - 24] with pyridinium phenol betaine-30, through careful determination of the absorption maximum and conversion into units of kilocalories per mole. The parameters for the dioxane–water mixtures were taken from the table of Reichardt and Dimroth [21] or interpolated from the values for mixtures not included in the table.

2.4. Spectroscopic measurements

The absorption spectra were obtained with a Cary model 17 spectrophotometer, and the fluorescence and phosphorescence spectra with a Perkin–Elmer Hitachi MPF-4 spectrofluorometer with an attachment for correcting spectra. The quantum yields were based on quinine sulfate in 0.1 N H_2SO_4 ($\phi_F = 0.55$). The sample temperatures were controlled at 25.0 ± 0.5 °C. The phosphorescence lifetimes were determined utilizing a Tektronix model 564 oscilloscope and a polaroid camera together with the MPF-4. The phosphorescence quantum yields were determined as follows. Solutions of the bimane sample and another solution containing either

9,10-diphenylanthracene or benzophenone were matched with respect to optical absorption densities. The emissions of the diethyl ether–pentane–ethanol (EPA) glasses prepared from the solutions were measured, and the phosphorescence quantum yields of the bimane obtained by comparing the areas under the emission curves for the bimane sample and the reference sample. The quantum yields of 9,10-diphenylanthracene ($\phi_F = 1$) [25] and benzophenone ($\phi_P = 0.74$) [26] were taken from the literature.

3. Results

3.1. Absorption spectra of 9,10-dioxabimanes

The position of the longest wavelength absorption band (solvent, dioxane) is very different for syn- and anti-bimanes: syn-bimanes, 354 - 395 nm ($\epsilon = 6500$ - 8000); diaryl-syn-bimanes, 409 and 415 nm ($\epsilon = 10\,000$ and $\epsilon = 10\,900$); anti-bimanes, 317 - 354 nm ($\epsilon = 11\,750$ - 18\,800). Absorption spectra for syn-$(CH_3,CH_3)B$ and anti-$(CH_3,CH_3)B$ are illustrated in Fig. 1. The effects of α-halogen, α-tert-butyl and α-phenyl groups on the position of the maxima are noteworthy [2].

A 4,6 bridge in syn-bimanes 3 $(X \equiv CY_2, NR, S)$ shifts the maxima to shorter wavelengths (from 327 to 345 nm); the unusually solvent-
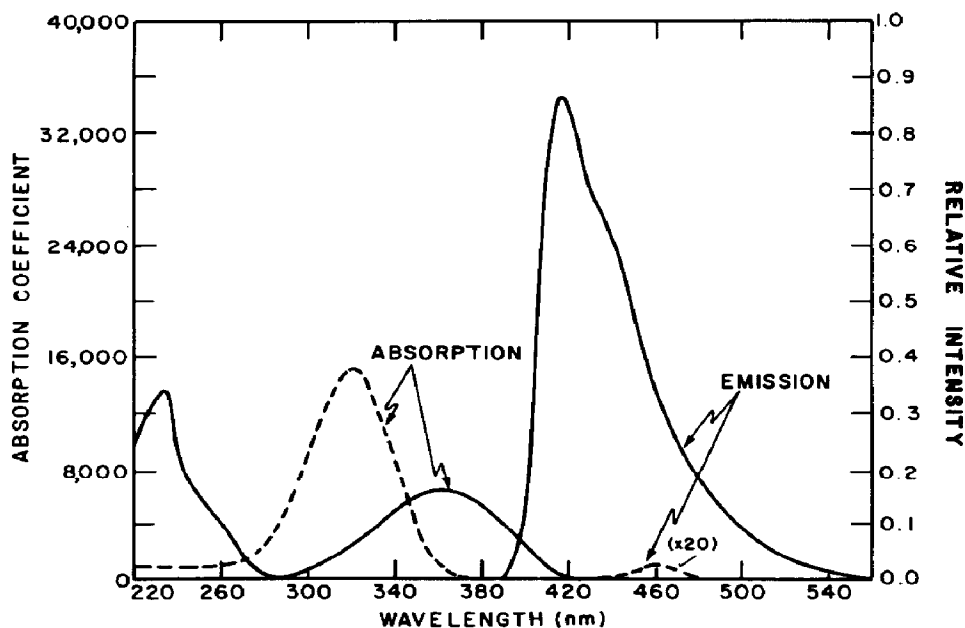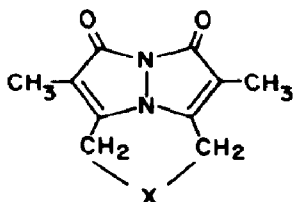

Fig. 1. Absorption and fluorescence spectra for syn-$(CH_3,CH_3)B$ (———) and anti-$(CH_3,CH_3)B$ (— — —) in dioxane. (The fluorescence emission curve for the anti-bimane has been amplified by a factor of 20.)

sensitive fluorescence quantum yields have been described in detail else-where [9].

Bridged <u>syn</u>-(-CH$_2$,CH$_3$)B

3

   Solvent polarity greatly influences the absorption maxima of the 9,10-dioxa-*syn*-bimanes; this is illustrated by roughly linear plots of the transition energies for *syn*-(CH$_3$,CH$_3$)B against the parameter $E_T(30)$ [21 - 24] (Fig. 2). (Further discussion on the selection of parameters is given in ref. 23; the nature of the solvent polarity parameters themselves is explained in ref. 24.) The absorption maxima of *anti*-bimanes are much less sensitive to solvent polarity, moving a little towards shorter wavelengths in polar solvents (Fig. 2).
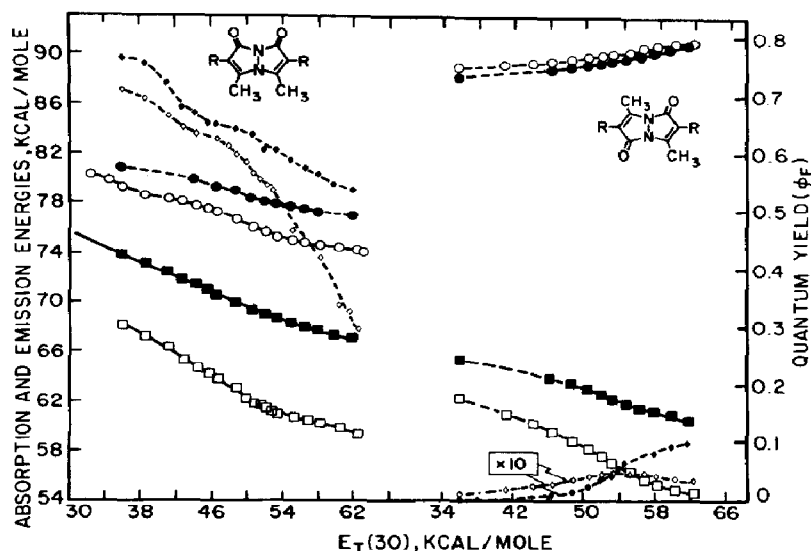

Fig. 2. Solvent polarity effects on the absorption and emission energies (in kilocalories per mole) and the fluorescence quantum yields ϕ_F for *syn*-(CH$_3$,CH$_3$)B, *syn*-(CH$_3$,H)B, *anti*-(CH$_3$,CH$_3$)B and *anti*-(CH$_3$,H)B are illustrated by plots against the parameter $E_T(30)$ (the ϕ_F value for the *anti* derivatives is multiplied by 10 for visibility): ●, ■, ◆, (CH$_3$,H)B derivatives; ○, □, ◇, (CH$_3$,CH$_3$)B isomers; ●, ○, absorption energies; ■, □, emission energies; ◆, ◇, fluorescence quantum yields.

3.2. Fluorescence spectra of 9,10-dioxabimanes

Syn-bimane fluorescence is usually strong (ϕ_F = 0.6 - 0.9 (solvent, dioxane)); anti-bimane fluorescence is normally weak (ϕ_F = 0.001 - 0.002 (solvent, dioxane)). The fluorescence spectra for syn- and anti-$(CH_3,CH_3)B$ are illustrated in Fig. 1. The 4,6-bridged bimanes show maxima around 430 nm (solvent, dioxane) with high quantum yields (greater than 0.7) unless the bridging group is a good electron donor [9]. The solvent polarity influences the fluorescence maxima more than the absorption maxima, as shown by the plots of the fluorescence emission energies against the solvent polarity parameter $E_T(30)$ (Fig. 2). The fluorescence spectra of the syn-bimanes in an EPA matrix at 77 K (Table 1) are very similar to those for dioxane solution at 298 K.

TABLE 1

Comparison of fluorescence and phosphorescence emissions from syn- and anti-9,10-dioxabimanes in ether:pentane:ethanol (5:5:2) matrices

Bimane	$\lambda_{max,F}$ [a] (nm)	$\lambda_{max,P}$ [a] (nm)	ϕ_P/ϕ_F [b]	τ_P (s)	ϕ_F [c]	ϕ_P [c]
9,10-dioxa-syn-bimane						
(CH_3,H)	392, 399, 414, 428 sh	475, 490, 514, 530 sh	0.01	1.95	0.88[d]	0.033
(CH_3,CH_3)	426, 450 sh	528, 565 sh	<0.01	1.05	0.75	0.004
$(-(CH_2)_4-)$	430, 450 sh	522, 565 sh	0.22	1.40		
$(CH_3,H) (CH_3,Cl)$	410, 430 sh	498, 535 sh	<0.01	0.90		
$(CH_3,CH_3) (CH_3,Cl)$	426, 455 sh	530, 570 sh	<0.01	0.50		
(CH_3,Cl)	426, 455 sh	530, 570 sh	<0.01	0.50	0.60	0.008
(CH_3,Br)	427, 450 sh	525, 565 sh	0.07	0.022	0.44	0.087
(CH_3,I)	435, 460 sh	530, 570 sh	0.32	0.0015	0.23	0.065
$(CH_3,(CH_3)_3C)$	423, 445 sh	515, 550 sh	<0.01	1.8		
(CH_3,C_6H_5)	464, 495 sh	565, 620 sh	<0.01	0.9		
(C_6H_5,CH_3)	449, 475 sh	575, 625 sh	<0.01	0.50		
$(4-ClC_6H_4,CH_3)$	448, 480 sh	575, 630 sh	0.11	0.85		
$(4-CH_3OC_6H_4,CH_3)$	449, 480 sh	575, 625 sh	0.034	0.80		
(C_6H_5,Cl)	449, 475 sh	573, 620 sh	0.023	0.30		
(C_6H_5,C_6H_5)	495, 530 sh	610, 670 sh	<0.01	0.60		
$(4-NO_2C_6H_4,C_6H_5)$	510, 550 sh	—	—	—		
9,10-dioxa-anti-bimane						
(CH_3,H)	—	444, 473 sh	$\rightarrow\infty$	0.95		0.45
(CH_3,CH_3)	—	480, 498 sh	$\rightarrow\infty$	0.50		0.30
$(-(CH_2)_4-)$	—	472, 492	$\rightarrow\infty$	0.50		
(CH_3,Cl)	—	480, 502 sh	$\rightarrow\infty$	0.20		0.29
(CH_3,Br)	—	480, 505 sh	$\rightarrow\infty$	0.008		0.35
(CH_3,C_6H_5)	—	524, 550 sh	$\rightarrow\infty$	0.1		
(C_6H_5,Cl)	—	524, 570, 620 sh	$\rightarrow\infty$	0.043		

[a] sh, shoulder.
[b] Determined from the relative heights of the respective emissions.
[c] Measured relative to benzophenone (ϕ_P for benzophenone, 0.74) ±10%.
[d] Measured relative to 9,10-diphenylanthracene (ϕ_F = 1) ±10%.

3.3. *Phosphorescence of 9,10-dioxabimanes in matrices*

9,10-dioxa-*syn*-bimanes are strongly fluorescent in EPA glass at 77 K; the phosphorescence can also be observed by chopping the short-lived fluorescence. The phosphorescences of *anti*-$(R_2,R_1)B$ are intense (ϕ_P values as high as 0.30 - 0.45). No fluorescence was observed for *anti*-bimanes in matrices at any temperature. The phosphorescence maxima for the bimanes are uncorrected; the true maxima are between 10 and 20 nm longer in wavelength.

The phosphorescence lifetimes of both 9,10-dioxabimanes are approximately 1 s in EPA at 77 K (that of the *syn* isomer is greater than that of the *anti* isomer) and are subject to heavy atom effects (the lifetime of *syn*-$(CH_3,I)B$ is 1.5 ms). The phosphorescence maxima, the relative quantum yields and the lifetimes of phosphorescence are listed in Table 1.

4. Discussion

Photophysical data for the 9,10-dioxabimanes constitute basic information on novel simple heterocyclic molecules consisting of two closely connected conjugated groups. The most important points relate to the striking differences between *syn*- and *anti*-bimanes. Four questions can be asked.

(1) Why does the absorption of *syn*-bimanes occur at considerably longer wavelengths than that of *anti*-bimanes?

(2) Why are *syn*-bimanes far more fluorescent than *anti*-bimanes?

(3) Why are the fluorescence maxima of 4,6-bridged *syn*-bimanes similar to those of unbridged *syn*-bimanes?

(4) Why are the solvent sensitivities of the absorption and fluorescence maxima of *syn*-bimanes similar and those of *anti*-bimanes different?

(1) The absorption maxima for *anti*-bimanes (325 nm) are similar to those of *cis*-s-*trans*-β-amino-α,β-unsaturated carbonyl compounds (300 - 330 nm ($\epsilon = 10\,000$ - $20\,000$)) [27]. The absorption maxima for the *syn* isomers (354 nm) reflect more conjugation in the π system.

X-ray studies reveal that *syn*-$(CH_3,CH_3)B$ and *syn*-(CH_3,H) are planar and *syn*-(C_6H_5,Cl) is almost planar (the dihedral angle around the N—N bond is 171.6°) in the crystal [28 - 31]. *Anti*-$(CH_3,H)B$ and *anti*-$(CH_3,CH_3)B$ are both planar but *anti*-$(C_6H_5,Cl)B$ deviates substantially from planarity (the dihedral angle around the N—N bond is 147.3°). The vertical nitrogen thermal parameters are larger (also those of the *anti* isomer are larger than those of the *syn* isomer) than might be accounted for by crystal packing effects [31]. These results suggest (a) that bimane molecules are flexible and (b) that 9,10-dioxa-*anti*-bimanes are less planar than the corresponding *syn* compounds.

Constraints in the crystal are relaxed for the molecules in solution; the bond arrangements around the central nitrogen atoms arise from (1) the tendency towards a tetrahedral arrangement (the bond orders around nitrogen are 3.7 or less [31]) and (2) nitrogen non-bonding electron avoidance, as in hydrazines and hydrazides [32] (for an earlier but compre-

hensive discussion on the conformational properties of hydrazines and hydrazides see ref. 33). Thus, non-planar bimanes ("twisted" *anti* (4) or "bent" *syn* (5) compounds) can be expected to predominate in solution.
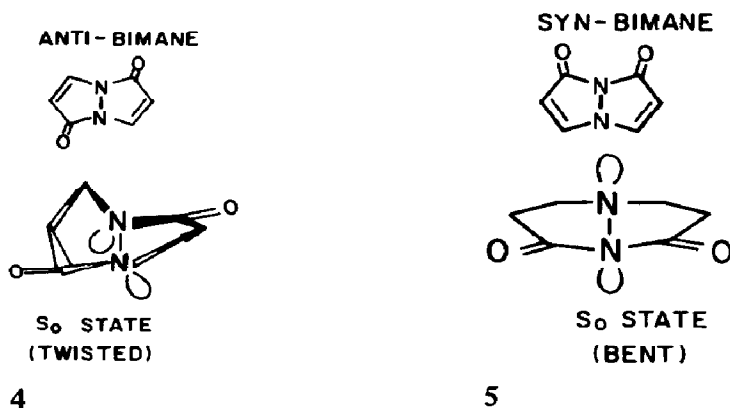
Twisted non-planar geometries for the *anti*-bimanes in solution, and more conjugated somewhat bent structures for *syn*-bimanes (a compromise between β-N overlap and nitrogen non-bonding orbital avoidance), account for the difference between the *syn*- and *anti*-bimane absorption maxima.

(2) Rapid intersystem crossing ($k_{isc} > 10^{11}$ s^{-1}) [14] accounts for the low fluorescence yield from *anti*-bimanes. It is more difficult to specify why the intersystem crossing rate is high, although considerable progress in ordering the electronic states of the *anti*-bimanes has been achieved [13].

(3) The μ-*syn*-bimanes (4,6-bridged *syn*-bimanes 3) absorb at shorter wavelengths than the unbridged *syn*-bimanes do but fluoresce at similar wavelengths (Table 2). The S_0 state of μ-*syn*-bimanes is strained (long bonds)

TABLE 2

Comparison of absorption and fluorescence maxima for bridged and unbridged *syn*-9,10-dioxabimanes in dioxane solution

Syn-(R_2, R_1)B	Dihedral angle [a] (deg)	Absorption[b], λ_{max} (nm)	Fluorescence[b], λ_{max} (nm)
(CH$_3$,H)	180	354	399
(CH$_3$,CH$_3$)	180	359	420
μ-(X)—(CH$_2$,CH$_3$)B			
—S—	141.8	344	430
—C(CN)$_2$—	139.3	331	426
—SO$_2$—	138.9	330	423
—N(CH$_3$)—	—	330	428
"Zero"	129.2	311	435

[a] Refs. 28 - 31.
[b] Ref. 4.

[28 - 31]. With more double-bond character in the bonds to the distal nitrogen atom (the atom far from the carbonyl groups) in the excited state, the S_1 state of a bridged compound would be less compressible than the S_1 state of a corresponding unbridged syn-bimane. The potential energy curves shown in Fig. 3 illustrate the relationships.

(4) The absorption and emission maxima of syn-bimanes change with solvent polarity like the absorption maxima of α,β-unsaturated ketones. In contrast, the absorption maxima of anti-bimanes shift to shorter wavelengths with increasing solvent polarity, probably because the dipole moments of the S_0 and Franck—Condon S_1 state are similar and small. The solvent sensitivity of the fluorescence maxima of the anti-bimanes implies a charge-separated emitting S_1 state, clearly different in charge distribution and possibly in electronic structure from the Franck—Condon S_1 state. The fluorescence lifetime (measured by picosecond techniques using a streak camera) found for anti-$(CH_3,H)B$ is 300 ps [34], a result which could imply a $^1n\pi^*$ emitting state. Further investigation is required to analyze the nature of the anti-bimane fluorescent state.
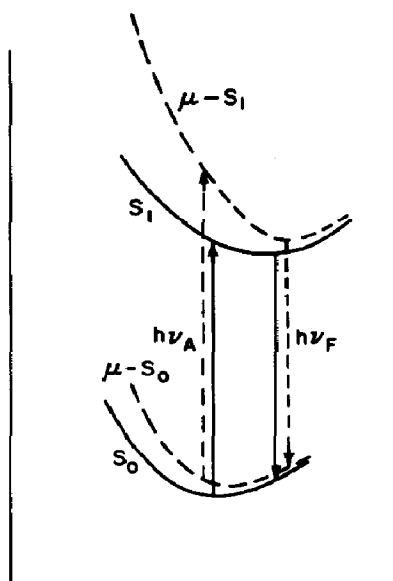

Fig. 3. Potential energy curves for the syn-bimanes (labeled S_0) and the μ-syn-bimanes (labeled μ-S_0) in both the ground and the excited states. The bridged bimane excited states will be more strained in the initial S_1 state but will relax to a level not very far from that of the unbridged syn-bimanes (see text).

4.1. Phosphorescence emissions

The phosphorescence lifetimes for both bimane isomers in a matrix at 77 K are long, from 0.5 to 2.0 s (that of the syn isomer is greater than that of the anti isomer), in the absence of heavy atom effects. Emission must thus occur from a $\pi\pi^*$ state. The only non-halogenated exception is anti-

$(CH_3, C_6H_5)B$, with a lifetime of 0.1 s, a value still clearly within the range expected for $\pi\pi^*$ emissions. The emitting $\pi\pi^*$ state (of *anti*-bimanes) is planar (optically detected magnetic resonance results [13]) but, to explain the rearrangement of the triplet to a lactone, a twisted triplet is required, as described in a separate paper [15].

5. Conclusion

The 9,10-dioxabimanes represent a broad new class of molecules with interesting and useful photophysical properties. Our studies provide some paradigms for not quite planar conjugated systems.

Acknowledgments

References

1 E. M. Kosower, B. Pazhenchevsky and E. Hershkowitz, *J. Am. Chem. Soc., 100* (1978) 6516.
2 E. M. Kosower and B. Pazhenchevsky, Bimanes 5, *J. Am. Chem. Soc., 102* (1980) 4983 - 4993.
3 E. M. Kosower, B. Pazhenchevsky, H. Dodiuk, H. Kanety and D. Faust, Bimanes 6, *J. Org. Chem., 46* (1981) 1666 - 1673.
4 E. M. Kosower, B. Pazhenchevsky, H. Dodiuk, M. Ben-Shoshan and H. Kanety, Bimanes 7, *J. Org. Chem., 46* (1981) 1673 - 1679.
5 N. S. Kosower, E. M. Kosower, G. L. Newton and H. M. Ranney, *Proc. Natl. Acad. Sci. U.S.A., 76* (1979) 3382 - 3386.
   N. S. Kosower, G. L. Newton, E. M. Kosower and H. M. Ranney, *Biochim. Biophys. Acta, 622* (1980) 201 - 209.
6 H. Gainer and N. S. Kosower, *Histochemistry, 68* (1980) 309 - 315.
   N. S. Kosower, E. M. Kosower, Y. Zipser, Z. Faltin and R. Shomrat, *Biochim. Biophys. Acta, 640* (1981) 748 - 759.
7 P. Wadsworth and R. D. Sloboda, *Biochemistry, 21* (1982) 21 - 28.
8 I. T. W. Matthews, R. S. Decker and C. G. Knight, *Biochem. J., 199* (1981) 611 - 617.
   I. T. W. Matthews, *J. Immunol. Methods, 51* (1982) 307 - 309.
9 E. M. Kosower, H. Dodiuk, H. Kanety and J. Hermolin, Bimanes 9, *J. Phys. Chem., 86* (1982) 1270.
10 E. M. Kosower, J. Hermolin, M. Ben-Shoshan and D. Faust, Bimanes 11, *J. Org. Chem., 46* (1981) 4578 - 4580.
11 D. Huppert, E. Pines, H. Kanety and E. M. Kosower, Bimanes 12, *J. Phys. Chem., 85* (1981) 3387 - 3391.

12 I. Goldberg and E. M. Kosower, Bimanes 13, *J. Phys. Chem.*, *86* (1982) 332 - 335.
13 H. Baba, N. Hirota and E. M. Kosower, *J. Phys. Chem.*, *85* (1981) 1469 - 1474.
14 D. Huppert, H. Dodiuk, H. Kanety and E. M. Kosower, *Chem. Phys. Lett.*, *65* (1979) 164.
15 H. Kanety, H. Dodiuk and E. M. Kosower, Bimanes 10, *J. Org. Chem.*, *47* (1982) 207 - 213.
16 E. M. Kosower, M. Ben-Shoshan, D. Faust and I. Goldberg, Bimanes 14, *J. Org. Chem.*, *47* (1982) 213 - 221.
17 P. Boldt, H. Militzer, W. Thielecke and L. Schulz, *Justus Liebigs Ann. Chem.*, *718* (1968) 101.
18 L. A. Carpino, P. H. Terry and S. D. Thatte, *J. Org. Chem.*, *31* (1966) 2867.
19 L. A. Carpino, *J. Am. Chem. Soc.*, *80* (1958) 601.
20 R. E. Buckles, M. P. Bellis and W. D. Coder, Jr., *J. Am. Chem. Soc.*, *73* (1951) 4972.
21 C. Reichardt and K. Dimroth, *Fortschr. Chem. Forsch.*, *11* (1968) 1.
   C. Reichardt, *Angew. Chem., Int. Edn. Engl.*, *18* (1979) 98 - 110.
22 E. M. Kosower, *J. Am. Chem. Soc.*, *80* (1958) 3253.
23 E. M. Kosower, H. Dodiuk and H. Kanety, *J. Am. Chem. Soc.*, *100* (1978) 4179.
24 E. M. Kosower, *An Introduction to Physical Organic Chemistry*, Wiley, New York, 1968.
25 R. Li and E. C. Lim, *J. Chem. Phys.*, *57* (1972) 605.
26 E. H. Gilmore, G. E. Gibson and D. S. McClure, *J. Chem. Phys.*, *20* (1952) 829; *23* (1955) 399.
27 J. V. Greenhill, *Chem. Soc. Rev.*, *6* (1977) 277.
28 E. M. Kosower, J. Bernstein, I. Goldberg, B. Pazhenchevsky and E. Goldstein, *J. Am. Chem. Soc.*, *101* (1979) 1620.
29 J. Bernstein, E. Goldstein and I. Goldberg, *Cryst. Struct. Commun.*, *9* (1980) 301.
   I. Goldberg, *Cryst. Struct. Commun.*, *9* (1980) 329.
30 I. Goldberg, J. Bernstein and E. M. Kosower, *Acta Crystallogr., Sect. B*, *38* (1982) 1990 - 2000.
31 I. Goldberg, J. Bernstein, E. M. Kosower, E. Goldstein and B. Pazhenchevsky, to be published.
32 M. Klessinger and P. Rademacher, *Angew. Chem., Int. Edn. Engl.*, *18* (1979) 826.
33 Y. Shvo, in S. Patai (ed.), *The Chemistry of the Hydrazo, Azo and Azoxy Groups*, Part 2, Wiley, New York, 1975, pp. 1017 - 1095.
34 K. Kaufman, D. Huppert and E. M. Kosower, unpublished results, 1980.